General theory of wave propagation through graded interfaces between positive- and negative-refractive-index media

Mariana Dalarsson[*]

Department of Physics and Electrical Engineering, Linnaeus University, 351 95 Växjö, Sweden

(Received 18 June 2017; published 20 October 2017)

The introduction of metamaterials and transformation optics has brought the possibilities for manipulating electromagnetic waves to an unprecedented level, suggesting applications like super-resolution imaging, cloaking, subwavelength focusing, and field localization. The refractive index of metamaterial structures in transformation optics typically has to be spatially graded. This paper presents a full analytical method for description of the field propagation through composites with gradient refractive index. The remarkable property of this approach is that it gives explicit general expressions for the field intensity and transmission and reflection coefficients, without reference to any boundary conditions. This opens a possibility for a novel fundamental theory of a number of important electromagnetic phenomena. The method enables calculation of wave propagation parameters within structures with arbitrary losses, arbitrary spectral dispersions, and arbitrary slopes of permittivity and permeability gradients, from mild to abrupt.

I. INTRODUCTION

One of the primary goals in electromagnetics is the manipulation of wavefronts of propagating and evanescent waves. A new degree of freedom is obtained if a spatial gradient of refractive index is introduced and interface phenomena are replaced by bulk effects. According to Fermat's principle, light travels through such materials along curved trajectories with the extreme value of optical path, usually the shortest [1,2]. This approach is the basis of gradient index lenses, the oldest examples being Maxwell's fish-eye and Luneburg lenses [3].

The problem with conventional optical materials is that the range of available values of the refractive index is limited to those found in nature. The introduction of electromagnetic metamaterials [4,5] enabled vast widening of that range. Subwavelength structuring enables direct control of the resonant electromagnetic behavior of a material, thus allowing tailoring of its refractive index to values not readily found in nature, including very high, near-zero, and negative. Simultaneously, it ensures control over frequency dispersion. This led to the introduction of transformation optics [6,7], where one optical space is mapped into another.

The spatial gradient of the refractive index is necessary for a vast majority of the applications of transformation optics. A number of applications using the spatial gradient of metamaterial-containing media have been proposed. Some examples include super-resolution imaging [8,9] and hyperlensing [10], electromagnetic cloaking [6,11,12] and illusion optics [13], superabsorption [14] and optical black holes [15], and subwavelength focusing and extreme field localization [16]. Other proposed applications include beam shaping and directing [17], enhancement of nonlinear effects [18], etc. Graded metamaterials were proposed as the basis for analog optical computing [19] that can perform, e.g., spatial differentiation and integration. The same approach is valid throughout the electromagnetic spectrum. Besides to propagating waves, the concepts can be applied to evanescent waves as well. The possibility to efficiently couple evanescent and propagating waves was considered in Refs. [20–22].

At this point, it is important to emphasize that there are a number of major physical differences between graded interfaces and sharp interfaces. These differences are addressed in the literature [6–22] in detail, as described in the previous paragraph. These physical differences actually allow for realization of some entirely new applications which are not possible using structures with conventional sharp interfaces between positive-refractive-index media (PIM) and negative-refractive-index media (NIM) media. Since the main objective of the present paper is the analytical description of the fundamental concepts behind these exciting applications, it is not possible to include a detailed account of all them here. A reader interested in a detailed introduction to the physical differences between graded interfaces and sharp interfaces is therefore referred to Refs. [6–22].

The approaches utilized in transformation optics can be applied also to other fields where wave propagation occurs. This includes acoustics [23,24], heat flow control and thermodynamics [25], matter waves in quantum mechanics [26], gravity and celestial mechanics [27], etc.

Analytical approaches to the calculation of wave propagation in graded metamaterial-containing structures are of special interest since they ensure fast, simple, and direct determination of the field distribution and the calculation of the wave propagation parameters [28–32]. A convenient mathematical form to describe interfaces between PIM and NIM is by a weighted tangent hyperbolic, since it can be used to describe a range of graded interfaces, from mild to abrupt ones. Previous analytical solutions for the field propagation through graded interfaces were limited to the case of constant impedance throughout the structure, and consequently without reflection [30–32].

In this paper, we present a complete analytical solution of Helmholtz' equation for the wave propagation through lossy graded metamaterial structures, where the dielectric permittivity and magnetic permeability can be described by hyperbolic-tangent functions and are generally independent of each other. Contrary to our previous considerations, we assume

---

[*]Corresponding author: mariana.dalarsson@lnu.se
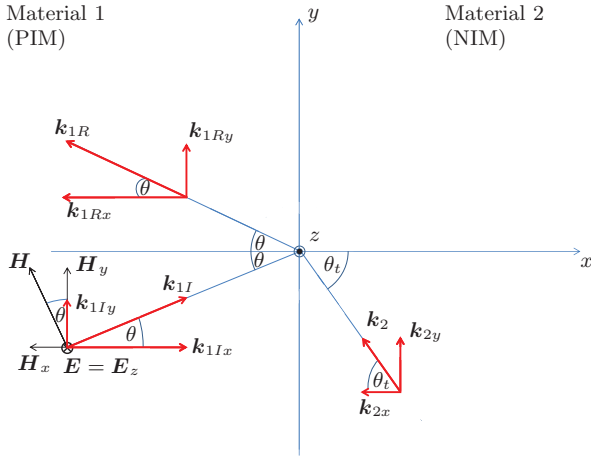
FIG. 1. Oblique incidence on an interface between the positive-refractive-index media (PIM) and the negative-refractive-index media (NIM).

general hyperbolic-tangent spatial gradients of the permittivity and permeability functions, and thus take reflections between the two media into account. We determine explicit relations for the field intensities and reflection and transmission coefficients across the structure, and show that they reproduce the well-known results in the limit of abrupt transition.

II. FIELD EQUATIONS

We start our analysis with the Maxwell equations in their differential form. The only assumptions we introduce at this point is that the fields are monochromatic and periodic in time, depending on $\exp(i\omega t)$, and that the mesoscopic material properties can be expressed by effective dielectric permittivity and effective magnetic permeability. In the case of metamaterials this assumption is valid, since the structuring of metal and dielectrics to obtain negative refraction must be at the subwavelength level so that the effective representation holds at dimensions comparable to the wavelength. The geometry of the problem is illustrated in Fig. 1.
The electric field strength vector is directed along the z axis, while the magnetic field vector is in the xy plane as indicated in Fig. 1, and we can write

$$\boldsymbol{H} = H(x,y)\cos\theta\,\hat{\boldsymbol{y}} - H(x,y)\sin\theta\,\hat{\boldsymbol{x}}, \quad \boldsymbol{E} = -E(x,y)\hat{\boldsymbol{z}}. \quad (1)$$

Thus the incident wave propagates along the direction of the $\boldsymbol{k}_{1I}$ vector, as shown in Fig. 1. The material properties vary along the x axis only, and we have $\epsilon = \epsilon(\omega,x)$ and $\mu = \mu(\omega,x)$. By keeping this in mind and substituting (1) into the curl equations,

$$\nabla\times\boldsymbol{E} = -i\omega\mu\boldsymbol{H}, \quad \nabla\times\boldsymbol{H} = i\omega\epsilon\boldsymbol{E}, \quad (2)$$

we obtain three scalar equations for the field intensities:

$$\frac{\partial E}{\partial y} = -i\omega\mu H\sin\theta, \quad \frac{\partial E}{\partial x} = -i\omega\mu H\cos\theta, \quad (3)$$

$$\frac{\partial H}{\partial x}\cos\theta + \frac{\partial H}{\partial y}\sin\theta = -i\omega\epsilon E. \quad (4)$$

Substituting the equations (3) into (4), we obtain the following equation for the electric field intensity:

$$\frac{\partial^2 E}{\partial^2 x} + \frac{\partial^2 E}{\partial^2 y} - \frac{1}{\mu}\frac{\partial\mu}{\partial x}\frac{\partial E}{\partial x} + \omega\mu\epsilon E = 0. \quad (5)$$

It is generally sufficient to solve Eq. (5) for the electric field intensity, since the magnetic field intensity can then easily be obtained from any of the two equations (3). It should be noted that in the present analysis, we have assumed transverse electric polarization for the oblique wave incidence. However, the case of transverse magnetic polarization can be treated in a fully analogous way, in which case we solve an equation analogous to (5) for the magnetic field intensity and then the electric field intensity can be easily obtained from either of the equations analogous to (3).

III. SOLUTIONS OF THE FIELD EQUATIONS

The temporal dispersions of the two materials and the gradual transition between them is described by means of the two functions $\epsilon = \epsilon(\omega,x)$ and $\mu = \mu(\omega,x)$. The spatial dependence of these two functions can be studied using various spatial functions, but the most suitable one is the hyperbolic-tangent function, as it provides correct asymptotic values in both materials and allows a detailed study of the limit of the abrupt transition as well. Thus, by means of such a model, it is possible to study the effects of the gradual transition between the two media. We therefore choose the following general functions:

$$\mu(\omega,x) = \mu_0\mu_r(\omega,x), \quad \epsilon(\omega,x) = \epsilon_0\epsilon_r(\omega,x), \quad (6)$$

with

$$\mu_r(\omega,x) = \frac{1}{2}(\mu_1 + \mu_2) - \frac{1}{2}(\mu_1 - \mu_2)\tanh\frac{x}{x_0}, \quad (7)$$

$$\epsilon_r(\omega,x) = \frac{1}{2}(\epsilon_1 + \epsilon_2) - \frac{1}{2}(\epsilon_1 - \epsilon_2)\tanh\frac{x}{x_0}, \quad (8)$$

where x_0 is a length parameter that determines the slope of transition, or the thickness of the graded interface, between the two materials. The smaller x_0 the more abrupt is the transition, as shown in Fig. 2. Using now the above assumption that the structuring of metal dielectrics to obtain negative refraction must be at the subwavelength level, substituting Eqs. (6)–(8) into Eq. (5) and separating the variables, we obtain a complete analytic solution of Eq. (5) as follows:

$$E(x,y) = E_0\frac{\Gamma(p+q+s)\Gamma(p+q-s+1)}{\Gamma(2p+1)\Gamma(2q)}$$
$$\times (1 + e^{2x/x_0})^{-i\frac{k_2 x_0}{2}\cos\theta_t}(1 + e^{-2x/x_0})^{-i\frac{k_1 x_0}{2}\cos\theta}$$
$$\times F\left(p+q+s, p+q-s+1, 2p+1; \frac{1}{1+e^{2x/x_0}}\right)$$
$$\times e^{-ik_2 y\sin\theta_t}, \quad (9)$$

where Γ is the Gamma function, $F(a,b,c;z)$ is the ordinary Gaussian hypergeometric function $_2F_1(a,b,c;z)$ represented by the hypergeometric series, and E_0 is the amplitude of the incident electric field, far to the right from the graded interface at $x = 0$. We also have the incident angle θ and the transmitted
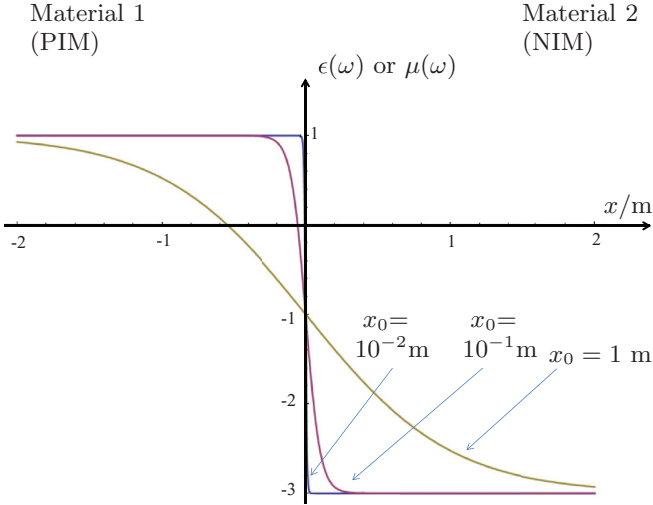
FIG. 2. Examples of transition profiles for different values of x_0.

angle θ_t with the minus signs, which are related to each other by Snell's law of refraction

$$k_1 \sin\theta = k_2 \sin\theta_t \Rightarrow n_1 \sin\theta = |n_2| \sin\theta_t, \qquad (10)$$

with k_1 and k_2 being the magnitudes of the wave vectors in the two materials far away from the transition plane ($|x| \gg x_0$). It should be noted here that we have not *a priori* assumed the Snell's law of refraction (10) in deriving our solution. Instead, Snell's law follows naturally from the geometry in Fig. 1 and the asymptotic forms of the solution (9). If losses in the two materials are neglected, then both k_1 and k_2 are real and positive quantities related to n_1 and n_2, the refraction indices of the two materials, respectively. Here we note that we have compensated for the negative sign of the refraction index n_2 in the negative-index part by a suitable convention for the transmission angle ($\theta_t \to -\theta_t$), as can be seen in Fig. 1. In the case that losses are included, which is particularly important for NIM where they cannot be neglected, then k_1 and k_2 are complex numbers defined using the same convention. In Eq. (9), we also introduced the following parameters:

$$p = -i\frac{k_2 x_0}{2}\cos\theta_t, \quad q = -i\frac{k_1 x_0}{2}\cos\theta,$$

$$s = \sqrt{r^2 + \frac{1}{4}} + \frac{1}{2}, \qquad (11)$$

with

$$r^2 = -\frac{\omega^2 x_0^2}{4c^2}(\mu_1 - \mu_2)(\epsilon_1 - \epsilon_2). \qquad (12)$$

The analytical result (9) is quite general and valid in the entire space. The analysis of the asymptotic behavior of (9) for $x \to +\infty$ (negative-index part) and $x \to -\infty$ (positive-index part) gives the following results for the Fresnel transmission and reflection coefficients for the structure described in Fig. 1:

$$\tau = \frac{\Gamma(p+q+s)\Gamma(p+q-s+1)}{\Gamma(2p+1)\Gamma(2q)},$$

$$\rho = \frac{\Gamma(p+q+s)\Gamma(p+q-s+1)\Gamma(-2q)}{\Gamma(p-q-s+1)\Gamma(p-q+s)\Gamma(2q)} \qquad (13)$$

It is now of interest to study these coefficients in the limit of abrupt transition ($x_0 \to 0$). In this limit we see from (12) that r^2 is second order in the small parameter x_0 and that (to the first order in x_0) it can be neglected altogether. Thus we have $s \to 1$, $p \ll 1$, $q \ll 1$. Using now the property of the Γ functions $\Gamma(z+1) = z\Gamma(z)$ and the asymptotic expansion of $1/\Gamma(z)$ given in Ref. [33], i.e., with

$$\frac{1}{\Gamma(z)} = \sum_0^\infty c_k z^k, \quad c_1 = 1 \Rightarrow \frac{1}{\Gamma(z)} \to z, \quad z \ll 1, \qquad (14)$$

as well as the definitions (11), we obtain the well-known results for the Fresnel transmission and reflection coefficients in the special case of abrupt transition,

$$\tau = \frac{2\eta_1 \cos\theta}{\eta_1 \cos\theta + \eta_2 \cos\theta_t}, \quad \rho = \frac{\eta_1 \cos\theta - \eta_2 \cos\theta_t}{\eta_1 \cos\theta + \eta_2 \cos\theta_t}, \qquad (15)$$

where η_1 and η_2 are the wave impedances of the positive- and negative-index media, respectively. Thus we see that in the special case of the abrupt transition, our results readily reproduce the well-known results (15) without reference to any boundary conditions between the two materials. However, the more general results (13) can also be used for graded transitions with different values of the length parameter x_0, being a measure of the size of the graded transition region between the two materials.

IV. NUMERICAL RESULTS

The general result (9) can be used to describe the propagation over the interface between positive- and negative-refractive-index media for electromagnetic waves of any frequency, as long as the mesoscopic properties of both materials can be expressed by their respective effective dielectric permittivities and effective magnetic permeabilities. We illustrate the present results using a case of wave propagation in the microwave range. In Figs. 3–5, we assume a lossy transmission with $f = 600$ MHz ($\lambda = 0.5$ m), $E_0 = 1$, $\epsilon_1 = 1 - 0.02i$, $\mu_1 = 1 - 0.01i$, $\epsilon_2 = -2.5 - 0.125i$, $\mu_2 = -1.6 - 0.04i$, and $x_0 = 0.25$ m. Note here that the chosen thickness x_0 of the graded transition region is not small, but rather is the size of half a wavelength. The electric field intensities $E(x, y)$ for four different incident angles ($\theta = \pi/4$, $\theta = \pi/6$, $\theta = \pi/12$, and $\theta = 0$) are shown in Fig. 3. From Fig. 3 we readily see that the transmitted waves in the metamaterial composite (LHM) to the right of the material boundary indeed propagate with the reverse direction of the wave vector and with correct transmission angles that are expected for metamaterial composites. The scales ($-2 \leqslant x, y \leqslant +2$) in Figs. 3(a) and 3(b) are different from the scales ($-1 \leqslant x, y \leqslant +1$) in Figs. 3(c) and 3(d), in order to better illustrate the different transmission angles. This choice of scales does not imply any physical difference between the two sets of graphical results.

In the present approach, the well-known property of wave-vector reversal in metamaterials follows naturally from the analytical solutions of Maxwell's equations without any *a priori* assumptions, except for negative values of the real parts of the relative permittivity and permeability functions as input parameters. Thus the present theory, based solely on

(a)

(b)

(c)

(d)
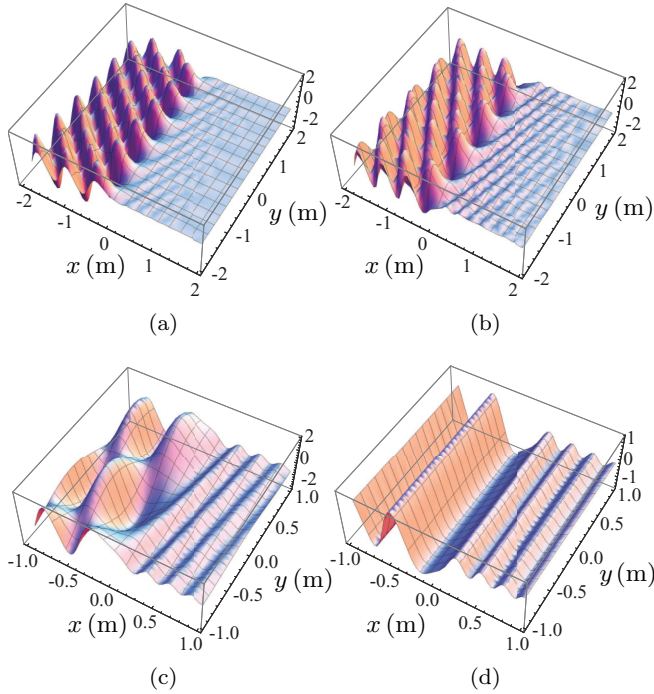
FIG. 3. The real part of the electric field intensity function $E(x,y)$ [V/m] given by (9) for incident angles (a) $\theta = \pi/4$, (b) $\theta = \pi/6$, (c) $\theta = \pi/12$, and (d) $\theta = 0$.

analytical solutions of the regular Maxwell equations, confirms the well-known behavior of metamaterial composites.

In order to make the different properties of the results presented in Fig. 3 more apparent, in Fig. 4 we show the cross sections of the same functions in the plane $y = 0$. From the results in Fig. 4, we see that for the given set of parameters and increased incident angles, the amplitude of the transmitted electromagnetic wave into the NIM decreases as expected. The wave into the NIM to the right of the boundary between the two materials is purely a transmitted wave, while the wave pattern

(a)

(b)

(c)

(d)
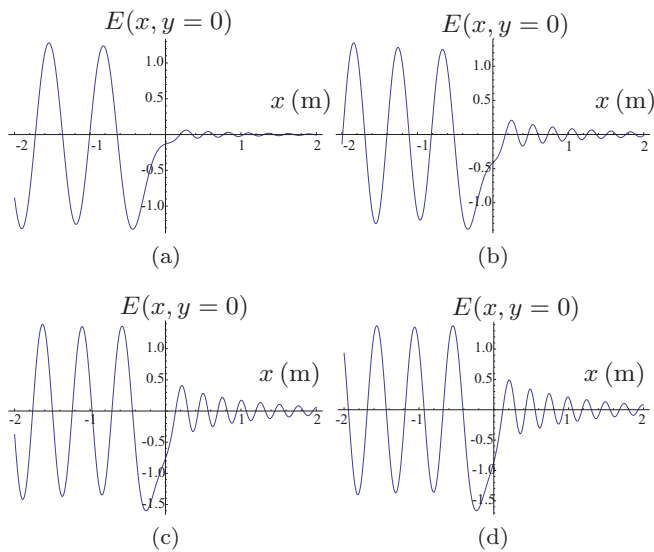
FIG. 4. The real part of the electric field intensity function $E(x,y=0)$ [V/m] given by (9) for incident angles (a) $\theta = \pi/4$, (b) $\theta = \pi/6$, (c) $\theta = \pi/12$, and (d) $\theta = 0$.

(a)

(b)

(c)
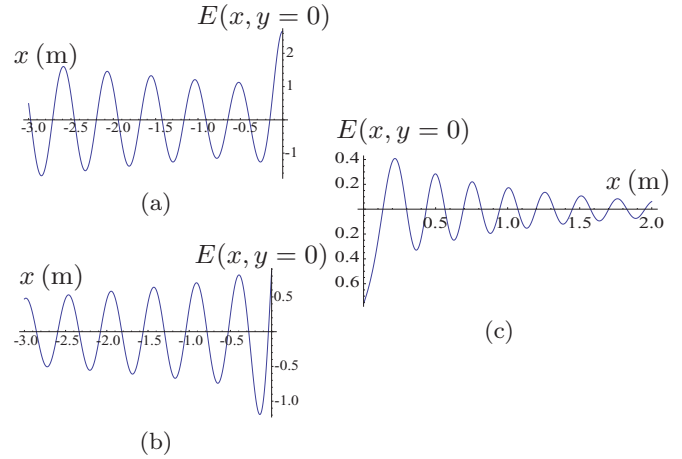
FIG. 5. Incident (a), reflected (b), and transmitted (c) waves for a lossy wave transmission with $\theta = \pi/12$.

in the positive-index media to the left of the boundary is a superposition of the incident wave and reflected wave. Using the transformation properties of the hypergeometric functions, it is possible to visualize the incident reflected and transmitted waves separately, as shown for $\theta = \pi/12$ in Fig. 5. From the wave patterns in Fig. 5, we see that far from the boundary, the incident and reflected waves behave as simple sinusoidal plane waves, as expected. Thus, using the asymptotic properties of the hypergeometric functions, we obtain the well-known asymptotic solutions

$$E(x,y) \rightarrow E_0\{\exp[-ik_1(x\cos\theta + y\sin\theta)]$$
$$+ R\exp[-ik_1(-x\cos\theta + y\sin\theta)]\},$$
$$x \rightarrow -\infty \tag{16}$$
$$E(x,y) \rightarrow E_0 T\{\exp[-ik_2(-x\cos\theta_t + y\sin\theta_t)]\},$$
$$x \rightarrow +\infty \tag{17}$$

where we note the reverse direction of the wave vector in the NIM, which arises naturally as a result of the analytical solution of the Maxwell equations (9). In the vicinity of the graded boundary, the wave patterns become distorted and there is a less clear distinction between the incident and reflected waves. However, the superposition of the two waves is well behaved, as can be seen from Fig. 4. Thus, the deviations in the incident and reflected waves are approximately equal and opposite to each other such that they cancel each other, as can be seen in Figs. 5(a) and 5(b) near the boundary $(x = 0)$.

In the above graphs, it is easy to compare the results obtained for graded interfaces to the regular results for sharp interfaces. In fact, for sharp interfaces the sinusoidal shape of the waves, as described by the asymptotic results (16) and (17), is observed throughout the structure, including the transition region around the boundary plane $(x = 0)$. Contrary to the conventional wave shapes for graded interfaces, we observe transition phenomena about the boundary plane $(x = 0)$ and the wave shapes deviate from the sinusoidal shapes obtained using the sharp interface analysis. These deviations are quite distinctly visible in Fig. 4, in particular in Figs. 4(a) and 4(b). These deviations constitute the basis for a number of

new physical phenomena, as described in Refs. [6–22]. An important feature of graded interfaces is that wave shapes can be artificially changed to fit the needs of a particular application by varying the grading properties of the interface. It is also important to note that the formulas (13) indeed include (15) as important special cases, but that (13) are much more general and allow for analytical calculation of the transmission parameters even when the transition is very smoothly graded.

Although the analysis in the present paper focuses on the case of double negative-refractive-index media, the analytical methods developed here can readily be generalized to both single negative cases and even to graded transitions between two ordinary PIM media. Such applications are, however, less common in the literature. Furthermore, as it is pointed out in the Introduction, although the present paper is concerned with propagating waves, the general solution (9) can readily be adapted to include the evanescent waves by replacing the appropriate real parameters by their imaginary counterparts. Thus, evanescent waves can also be included in the present method. However, it requires a careful algebraic redesign of the solution, which is not the subject of the present study.

V. CONCLUSIONS

We have investigated electromagnetic wave propagation across a graded interface between positive-refractive-index media and negative-refractive-index media, in a general case where the material parameters of the two media are independent from each other, thus taking reflections into account. We derived and analyzed a general analytical result for the electric field intensity and the transmission and reflection coefficients, for the case of oblique incidence with transverse electric polarization. The transverse magnetic case can be solved as well using an analogous approach. Thereby we have shown that all the fundamental properties of metamaterial composites readily follow from the analytical solution for the electric field intensity in the entire space, without reference to any boundary conditions or *a priori* assumptions. We believe that the results presented in the present paper constitute an important step towards a new paradigm in our fundamental theoretical description of the electromagnetic wave propagation over interfaces between positive- and negative-refractive-index media, applicable to a majority of practical situations that arise in the field.

[1] M. Born and E. Wolf, *Principles of Optics*, 7th ed. (Cambridge University Press, Cambridge, UK, 1999).

[2] U. Leonhardt and T. G. Philbin, Prog. Opt. **53**, 69 (2009).

[3] E. W. Marchand, *Gradient Index Optics* (Academic Press, New York, 2012).

[4] W. Cai and V. Shalaev, *Optical Metamaterials: Fundamentals and Applications* (Springer, Dordrecht, 2009).

[5] S. A. Ramakrishna and T. M. Grzegorczyk, *Physics and Applications of Negative Refractive Index Materials* (SPIE Press, Bellingham, WA and CRC Press, Taylor and Francis Group, Boca Raton, FL, 2009).

[6] J. B. Pendry, D. Schurig, and D. R. Smith, Science **312**, 1780 (2006).

[7] U. Leonhardt, Science **312**, 1777 (2006).

[8] S. A. Ramakrishna and J. B. Pendry, Phys. Rev. B **69**, 115115 (2004).

[9] N. Kundtz and D. R. Smith, Nat. Mater. **9**, 129 (2010).

[10] Z. Jacob, L. V. Alekseyev, and E. Narimanov, Opt. Express **14**, 8247 (2006).

[11] W. Cai, U. K. Chettiar, A. V. Kildishev, and V. M. Shalaev, Nat. Photon. **1**, 224 (2007).

[12] J. Valentine, J. Li, T. Zentgraf, G. Bartal, and X. Zhang, Nat. Mater. **8**, 568 (2009).

[13] Y. Lai, J. Ng, H. Y. Chen, D. Z. Han, J. J. Xiao, Z.-Q. Zhang, and C. T. Chan, Phys. Rev. Lett. **102**, 253902 (2009).

[14] J. Ng, H. Chen, and C. T. Chan, Opt. Lett. **34**, 644 (2009).

[15] E. E. Narimanov and A. V. Kildishev, Appl. Phys. Lett. **95**, 041106 (2009).

[16] H. A. Atwater and A. Polman, Nat. Mater. **9**, 205 (2010).

[17] I. V. Shadrivov, A. A. Sukhorukov, and Y. S. Kivshar, Appl. Phys. Lett. **82**, 3820 (2003).

[18] T. H. Fung, L. L. Leung, J. J. Xiao, and K. W. Yu, Opt. Commun. **282**, 1028 (2009).

[19] A. Silva, F. Monticone, G. Castaldi, V. Galdi, A. Alù, and N. Engheta, Science **343**, 160 (2014).

[20] M. Kadic, S. Guenneau, and S. Enoch, Opt. Express **18**, 12027 (2010).

[21] Y. Liu, T. Zentgraf, G. Bartal, and X. Zhang, Nano Lett. **10**, 1991 (2010).

[22] S. Sun, Q. He, S. Xiao, Q. Xu, X. Li, and L. Zhou, Nat. Mater. **11**, 426 (2012).

[23] H. Chen and C. T. Chan, J. Phys. D **43**, 113001 (2010).

[24] L. Zigoneanu, B. I. Popa, and S. A. Cummer, Nat. Mater. **13**, 352 (2014).

[25] S. Guenneau, C. Amra, and D. Veynante, Opt. Express **20**, 8207 (2012).

[26] S. Zhang, D. A. Genov, C. Sun, and X. Zhang, Phys. Rev. Lett. **100**, 123002 (2008).

[27] D. A. Genov, S. Zhang, and X. Zhang, Nat. Phys. **5**, 687 (2009).

[28] A. O. Pinchuk and G. C. Schatz, J. Opt. Soc. Am. A **24**, A39 (2007).

[29] N. M. Litchinitser, A. I. Maimistov, I. R. Gabitov, R. Z. Sagdeev, and V. M. Shalaev, Opt. Lett. **33**, 2350 (2008).

[30] M. Dalarsson and P. Tassin, Opt. Express **17**, 6747, (2009).

[31] M. Dalarsson, M. Norgren, N. Dončov, and Z. Jakšić, J. Opt. (Bristol, UK) **14**, 065102 (2012).

[32] M. Dalarsson, M. Norgren, T. Asenov, N. Dončov, and Z. Jakšić, J. Nanophoton. **7**, 073086 (2013).

[33] *Handbook of Mathematical Functions, with Formulas, Graphs, and Mathematical Tables*, edited by M. Abramowitz and I. A. Stegun, Applied Mathematics Series 55 (Dover Publications, New York, 1964).